Kornerupine breakdown reactions in paragneisses from southern Madagascar

DIETRICH ACKERMAND

Mineralogisch-Petrographisches Institut, Universität, Olshausenstr. 40, 2300 Kiel, Germany

BRIAN F. WINDLEY

Department of Geology, The University, Leicester LE1 7RH, U.K.

AND

ANDRIANTEFISON H. RAZAFINIPARANY

Service de Géologie, Université, Antananarivo, Madagascar

Abstract

Kornerupine-rich layers up to several centimetres thick with minor sillimanite, spinel, Fe oxide and ilmenite occur in a diopsidite in sillimanite–cordierite gneiss south of Beraketa (24°27′S, 46°48′E), southern Madagascar. Kornerupine, sillimanite, spinel and hematite grains up to 1 mm across have mutual polygonal boundaries indicating textural equilibrium at their crystallisation. Kornerupine has X_{Mg} 0.67–0.80 and 0.9 to 2.6 wt.% B_2O_3. Sillimanite contains up to 2.0 wt.% Fe_2O_3. Spinel is essentially $(Mg,Fe^{2+})\ Al_2O_4$ with an X_{Mg} range of 0.29–0.40 and exsolution lamellae of Fe oxide. Textural relations demonstrate two limited reactions, each confined to areas less than 500 μm across: (1) Kornerupine and spinel reacted along grain contacts to form very fine-grained tourmaline, corundum and chlorite. The replacing phases are symmetrically zoned with a central tourmaline and hematite, bordered by an aggregate of chlorite, tourmaline and corundum, followed outwards by a rim of chlorite against the kornerupine and spinel. (2) Within kornerupine grains, zoned, round aggregates consist of very fine-grained chlorite, tourmaline and corundum of different composition than in (1). They define the terminal reaction of kornerupine breakdown.

Geothermobarometry indicates that the early kornerupine-bearing assemblage was stable at 7.0 kbar and 700 °C. This *P–T* point lies close to the retrograde, nearly isothermal trajectory defined independently by nearby sapphirine-bearing assemblages. The fine-grained aggregates formed most likely during further cooling, or by increasing water fugacity.

KEYWORDS: kornerupine, breakdown products, granulite facies, Madagascar.

Introduction

THE Precambrian of southern Madagascar consists largely of paragneisses with abundant garnet, sillimanite, and cordierite, locally with remarkable concentrations of Al and Mg represented by metre-thick layers of sillimanitite and cordieritite (Ackermand *et al.*, 1989). According to unpublished sources (T. Razakamana, pers. comm.) and the occurrences reported by Lacroix (1922–3), Megerlin (1968), von Knorring *et al.* (1969) and Nicollet (1988), within these paragneisses are centimetre-thick layers consisting almost entirely of kornerupine, with minor phases like sapphirine, spinel and sillimanite. We report here one such new kornerupine occurrence, together with the limited breakdown of kornerupine to chlorite, corundum and tourmaline, and ambient *P–T* conditions calculated from assemblages in adjacent rocks.

The aim of this paper is to document new examples of borosilicate-bearing reactions, and to understand the metamorphic conditions producing the large granoblastic–polygonal texture of kornerupine and the later fine-grained reaction products.

Geological background

The Precambrian geology of Madagascar was described by Besairie (1971) and Hottin (1976),

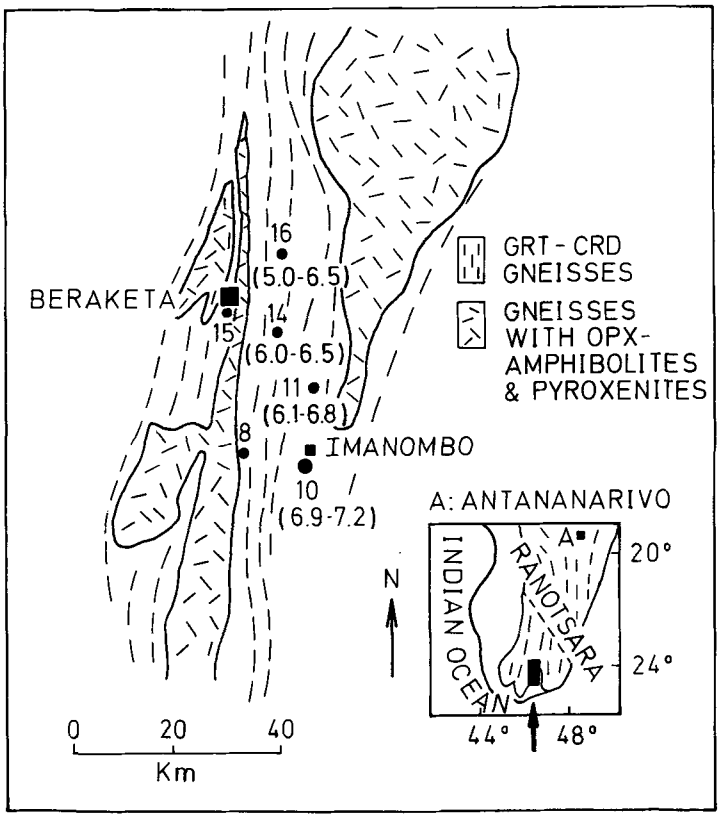

FIG. 1. Simplified geological map of southern Madagascar showing the position of the kornerupine-bearing occurrence at locality 10. Other numbers (in parentheses) refer to localities where *P–T* conditions have been calculated, in particular *P* values determined by cordierite–spinel–quartz barometry.

and relevant isotropic data reviewed by Cahen and Snelling (1984).

The Precambrian rocks of southern Madagascar, south of the Ranotsara shear belt (Fig. 1), have a north–south regional strike, and steep to vertical dip. There are several belts up to about 100 km wide, which have distinctive lithostratigraphies and metamorphic grade, and which are separated by major north–south shear zones.

The Beraketa belt (Noizet, 1969) is up to 20 km wide and 300 km long (Fig. 1), and consists of garnet–cordierite–sillimanite–spinel paragneisses partly of amphibolite but mainly of granulite facies. These gneisses contain layers of garnet–sillimanite–spinel-bearing quartzitic gneiss, diopsidite, sapphirine-phlogopitite in diopsidite, marbles and calc-silicates, cordieritite, sillimanitite, and transitional rock types, each up to several metres thick. Locally, these rocks are interlayered with charnockite, hypersthene amphibolite and pyroxenite of granulite-facies mineralogy. Phlogopite-bearing diopsidites contain coarse-grained pockets that typically consist of phlogopite (usually the major phase), sapphirine, cordierite, sillimanite, orthopyroxene, and sporadically wollastonite, anorthite, garnet, quartz, spinel, anhydrite, scapolite, titanite, carbonate, beryl and fluorite (Lacroix, 1941). Some diopsidites contain borosilicates such as kornerupine, tourmaline, grandidierite and serendibite (Nicollet, 1988), and sinhalite (our observation), and anatectic paragneisses (about 200 km to the north) contain grandidierite, serendibite and tourmaline (Nicollet, 1990).

In one of these pockets described above, which is about 50 cm across, layers up to 5 cm thick consisting almost entirely of kornerupine have been found for the first time about 2 km south of Imanombo and 37 km south-east of Beraketa (Fig.1, locality 10). The diopsidite with this kornerupine-bearing pocket (we found only one) is bordered by garnet–sillimanite–cordierite gneiss. The 1:500000 map of southern

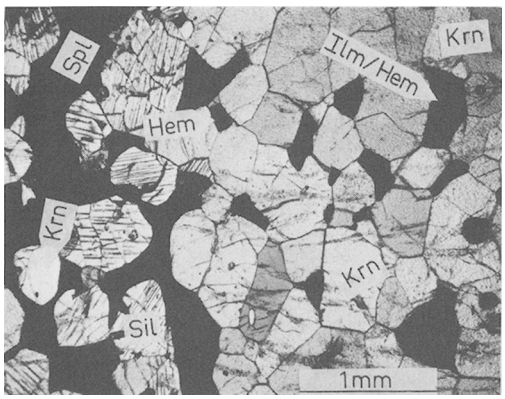

FIG. 2. Photomicrograph showing a central patch which contains a kornerupine-rich layer, and on the left a layer with sillimanite, spinel and ilmenite(/hematite) and kornerupine (specimen No. M10 IIIB).

Madagascar (Carte Geologique, No. 8—Ampanihysheet; Besairie, 1970) and the 1:50 000 Beraketa map sheet indicate the presence of sapphirine at this locality. We did not observe sapphirine, and suggest that blue (pleochroic) kornerupine was misidentified as sapphirine.

Mineral assemblages and textures

Kornerupine-rich rocks. The kornerupine-rich layers contain minor sillimanite, spinel, hematite and ilmenite, and locally mm-sized patches enriched in sillimanite, spinel and ilmenite (Fig. 2). Spinels exhibit exsolved bands of Fe oxide and some ilmenites have exsolved lamellae of hematite of two generations. Kornerupines, sillimanites, spinels and Fe–Ti oxides, in grains up to 1 mm across, form a granoblastic–polygonal mosaic, indicative of static equilibrium recrystallization.

We discuss two alterations observed in the kornerupine-bearing layers, each confined to areas less than 500 μm across:

(1) A limited breakdown of kornerupine and spinel, between which are found the phases chlorite, tourmaline and corundum (Fig. 3A). The spinel contains grains and exsolved bands of Fe oxide and also minor inclusions of corundum, which in turn contain idiomorphic grains of hematite (not seen in Fig. 3A). In the fine-grained alteration area there are two zoned structures, the centres of which consist of tourmaline and hematite with successive outward rims of hematite + corundum, radiating tourmaline + corundum, tourmaline with chlorite (bordering kornerupine) and chlorite (bordering spinel). The iron oxide cores are considered to represent original magnetite that had formed through early exsolution from spinel but did not take part in the later alteration of kornerupine and spinel.

These relations are explained in Fig. 3B and C, in which B shows the kornerupine and spinel (with its two inclusions of Fe-oxide) before the alteration, and C shows the altered area with the two zoned structures with the three other phases. These relations can be explained by the reaction:

$$\text{Krn} + \text{Spl} = \text{Chl} + \text{Tur} + \text{Crn} \qquad \text{(I)}$$

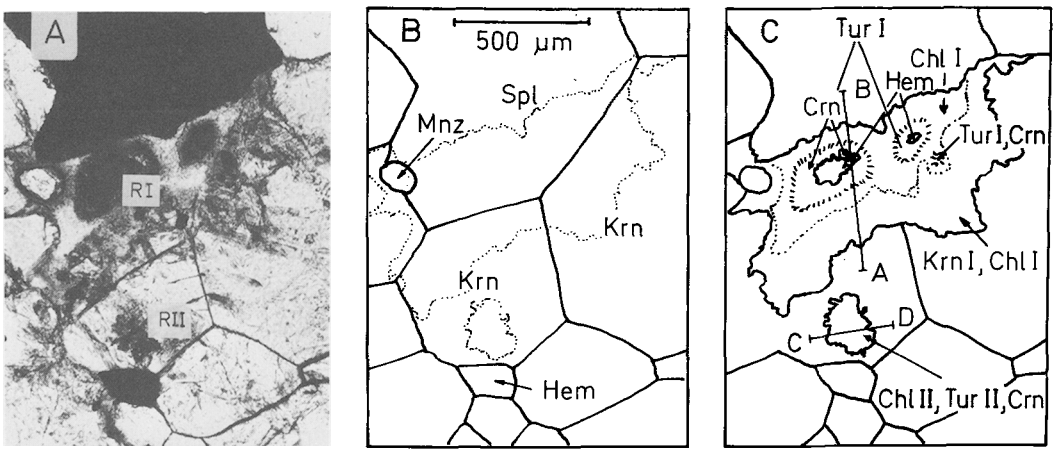

FIG. 3. The two kornerupine breakdown reactions R1 and R2 (specimen No. M10 IIIC; mineral symbols after Kretz, 1983; Mnz—monazite): A, photomicrograph showing the two kornerupine breakdown reaction areas; B, diagram illustrating the estimated position of the original kornerupine–spinel boundary before breakdown reaction 1 and the present reaction boundaries (dotted lines); C, diagram showing the reaction area 1 between the reactants kornerupine + spinel, and reaction area 2 within a kornerupine grain. A–B and C–D refer to reaction profiles marked in Fig. 5.

(2) Within some kornerupine grains there are zoned, round aggregates (see Fig. 3A) of chlorite, tourmaline, and corundum, with the chlorite bordering the kornerupine. These aggregates are typically not found in the margins of kornerupine grains, and these relations demonstrate the limited alteration of the kornerupine grains, according to the reaction:

$$\text{Krn} = \text{Chl} + \text{Tur} + \text{Crn} \qquad \text{(II)}$$

The reaction areas (I) and (II) occur bordering or within the same grain or in different grains. Although the above two reaction areas can be observed with the microscope, many of the reaction products can only be verified by the microprobe, because the grain sizes are between 10 and 0.5 μm across.

Mineral chemistry

Microprobe analyses were obtained with a Cameca Camebax-Microbeam and especially for boron with a Cameca SX 50. The working conditions were (5 kV, 15 nA, and a 0.5 μm beam diameter; the on-line correction program for quantitative element analyses was from Pouchou and Pichoir (1984).

Kornerupine-rich rocks. Representative point analyses of minerals from about 500 analyses are given in Table 1, and the range in composition of the reactants and products is depicted in Fig 4A and B.

Kornerupine. No regular zoning was observed from core to rim, an observation consistent with the absence of optical zoning. Clean kornerupine is compositionally almost homogeneous with 29.5 wt.% SiO_2, 1.0 wt.% B_2O_3, 41.5 wt.% Al_2O_3, 10.0 wt.% FeO and 14.0 wt.% MgO as average values. Exceptions are found in patches of grains with reaction areas. When comparing reaction areas (I) and (II), the Al_2O_3 contents (41.0 to 42.5 wt.%) vary inversely with those of B_2O_3 (2.6 to 0.9 wt.%), respectively; X_{Mg} varies from 0.80 to 0.67.

Sillimanite contains up to 2.0 wt.% Fe_2O_3 and up to 0.2 wt.% MgO. These values are high compared with those of sillimanites in other high-grade metamorphic rocks (Grew, 1980). Boron was not detected (<0.1 wt.%), although sillimanite may incorporate more than 0.1 wt.% B_2O_3 at high temperatures in a boron-rich environment at very low partial pressures of water (Grew and Hinthorne, 1983).

Spinel. From stoichiometry considerations, spinel is essentially $(MgFe^{2+})Al_2O_4$ with an X_{Mg} range from 0.29 to 0.40. The calculated Fe_2O_3 shows less than 1 mole % magnetite. No Zn was detected (<0.05 wt.%). Frequent exsolution lamellae in spinel consist of hematite, as suggested by the chemical composition. Optical data from large lamellae allow the assumption that the hematite is derived from magnetite.

Ilmenite contains patches of solid solution of (hemo-) ilmenite with exsolved lamellae of (ilmo) hematite and hematite ($TiO_2 < 0.04$ wt.%), indicating two generations of exsolution.

Reaction Products. Tourmaline, chlorite and corundum occur only in aggregates formed by the retrograde reaction. Three areas with reaction type I and five with reaction type II were selected for analyses of reaction products. Point analyses given in Table 1 and Fig. 4 are compositions which are supported by more than ten other point analyses taken from different areas and different grains. Fig. 4 shows that tourmaline I (reaction I, Tur I) has a wide range of values in comparison with tourmaline II (reaction II, Tur II), and furthermore that tourmaline II is richer in Al_2O_3 and SiO_2. Diadochy between Mg and Fe gives an X_{Mg} range from 0.42 to 0.63 for tourmaline I and with a constant value of ±0.69 for tourmaline II. Chlorite I (reaction I) has X_{Mg} from 0.68 to 0.36, whereas chlorite II (reaction II) varies less (0.68 to 0.74). Chlorite I also has a higher Al than chlorite II. In corundum Fe_2O_3 is high (up to 4.5 wt.%).

Associated rocks. Analyses were undertaken of the minerals in the cordieritite (Crd, Sil, Pl, Bt, Ilm and Fe oxides), Grt-gneiss (Grt, Sill, Qtz, Pl, Kfs, Bio, Spl, Ilm and Fe oxides), Grt-Crd-gneiss (Grt, Crd, Sil, Qtz, Pl, Kfs, Bt, Spl, Ilm and Fe oxides), and pyroxenite (Cpx, Opx, Hbl, Scp, Pl, Bt, Ilm and Fe oxides) (abbreviations, Kretz, 1983). These analyses (Table 2) were used for the *P–T* calculations.

Chemical profiles across reaction areas

In the kornerupine-bearing rocks the following reactions have been postulated above:

$$\text{Krn (I)} + \text{Spl} = \text{Ch I} + \text{Tur I} + \text{Crn} \qquad \text{(I)}$$

$$\text{Krn (II)} = \text{Chl II} + \text{Tur II} + \text{Crn} \qquad \text{(II)}$$

As supporting evidence for these reactions, we present the microprobe profiles Fig. 5A and B across the reacting and product phases. The Fe-intensity was counted every 1 μm. Reaction 1 is described by profile A–B (Fig. 5A). Homogeneous kornerupine is altered (Krn (I)) marginally towards the reaction area with variable concentrations of Al, Si, Mg and Fe. Also spinel shows a zonation of Al, Mg and Fe towards

Table 1. Representative mineral point analyses in the kornerupine-bearing layers

	Kornerupine			Spinel		Sil	Ilm	Tourmaline			Chlorite			Corundum
Nos.*	12	209	292	74	202	7	106	210	221	297	204	216	295	208/290
		Krn I	Krn II					Tur I	Tur I	Tur II	Chl I	CHL I	Chl II	
Area**	5/1-1	1/1-1	2/1 -1	5/2-8	1/2	5/3	5/4/1	1/3-1	1/3-12	2/2-1	1/4-1	1/4-3	2/3-1	1/5,2/4
SiO_2	29.36	29.41	29.45	-	-	36.26	-	31.08	34.66	35.70	21.72	24.31	26.58	0.03
B_2O_3	1.00	2.60	0.95			-		***	***	***				
TiO_2	0.13	0.13	0.10	-	0.02	0.03	48.89	0.12	0.05	0.06	0.02	0.06	-	0.02
Al_2O_3	41.26	41.05	42.02	61.75	59.32	61.48	0.03	35.12	35.96	37.12	27.98	26.21	23.77	95.75
Cr_2O_3	0.02	0.01	0.02	0.41	0.30	0.06	-	-	0.04	-	-	0.02	-	0.34
Fe_2O_3	not calculated					1.86	7.10	not calculated						4.31
FeO	9.83	9.72	10.55	28.95	30.15	-	41.85	11.58	6.40	5.91	28.40	22.59	16.79	-
MnO	0.42	0.43	0.41	0.55	0.47	-	1.82	0.04	0.02	0.02	0.23	0.19	0.20	0.07
MgO	13.90	13.82	13.85	8.39	9.09	0.12	0.15	5.26	6.06	7.12	9.83	15.95	20.86	0.19
CaO	0.04	0.02	0.04	0.02	-	-	-	1.42	1.27	1.17	-	-	0.01	-
Na_2O	0.10	0.09	0.05	0.02	0.02	-	-	1.38	1.50	1.32	0.04	0.06	0.02	0.01
K_2O	0.01	-	0.01	0.01	-	0.02	-	0.01	0.01	0.01	-	-	-	0.01
F****	0.15	0.14	0.12					-	-	-	-	-	-	
Total	96.22	97.42	97.57	100.10	99.37	99.83	99.84	86.01	85.97	88.43	88.22	89.39	88.23	100.73
Calculation basis (oxygens)	21.5			4		10	6	24.5			28			6
Si	3.851	3.774	3.820	-	-	1.975	-	5.257	5.652	5.635	4.622	4.934	5.296	0.001
B	0.226	0.576	0.212			-								
Ti	0.013	0.013	0.009	-	-	0.001	1.864	0.015	0.006	0.007	0.003	0.009	-	0.001
Al	6.379	6.209	6.424	1.982	1.936	3.946	0.002	7.001	6.911	6.905	7.018	6.269	5.582	3.869
Cr	0.002	0.001	0.002	0.009	0.007	0.003	-	-	0.005	-	-	0.003	-	0.009
Fe^{3+}	-	-	-	-	-	0.076	0.271	-	-	-	-	-	-	0.111
Fe^{2+}	1.078	1.043	1.144	0.659	0.698	-	1.774	1.638	0.873	0.780	5.055	3.834	2.798	-
Mn	0.047	0.047	0.045	0.012	0.011	-	0.078	0.006	0.003	0.002	0.042	0.033	0.034	0.002
Mg	2.718	2.644	2.678	0.341	0.375	0.010	0.011	1.326	1.473	1.675	3.118	4.825	6.195	0.010
Ca	0.006	0.003	0.006	0.001	-	-	-	0.257	0.222	0.198	-	-	0.002	-
Na	0.025	0.022	0.013	0.001	0.001	-	-	0.453	0.474	0.403	0.016	0.023	0.007	0.001
K	0.002	-	0.002	-	-	0.001	-	0.002	0.002	0.002	-	-	-	-
F	1.452	1.340	1.189					-	-	-	-	-	-	
X_{Mg}	0.716	0.717	0.692	0.336	0.349		0.006	0.447	0.628	0.680	0.382	0.555	0.686	

Total Fe usually calculated as FeO. In spinel only minor Fe^{3+}; "-" less than 0.01 wt.%; Cl less than 0.01 wt.% in Krn and Tur

*: EPMA point analysis number

**: "5/1-3" area 5, phase 1, 3rd point analysis on phase 1; "1/2" area 1 (example for reaction 1), phase 2; "2/3" area 2 (example for reaction 2), phase 3 etc.

***: B in Tur not analysed

****: Total includes O ≡ F.

the reaction area. The product phase bordering kornerupine and spinel is chlorite (Chl I), followed by a narrow zone of tourmaline + corundum aggregate, then a broad tourmaline (Tur I) aggregate which also contains corundum. The tourmaline aggregate shows lower Al and Fe and higher Si and Mg at the contact with the Fe oxide.

We have balanced the texturally observed reaction I, using the reaction coefficient program of Finger and Burt (1972) with the stoichiometric data of the five phases given in Table 1 (Krn (I),

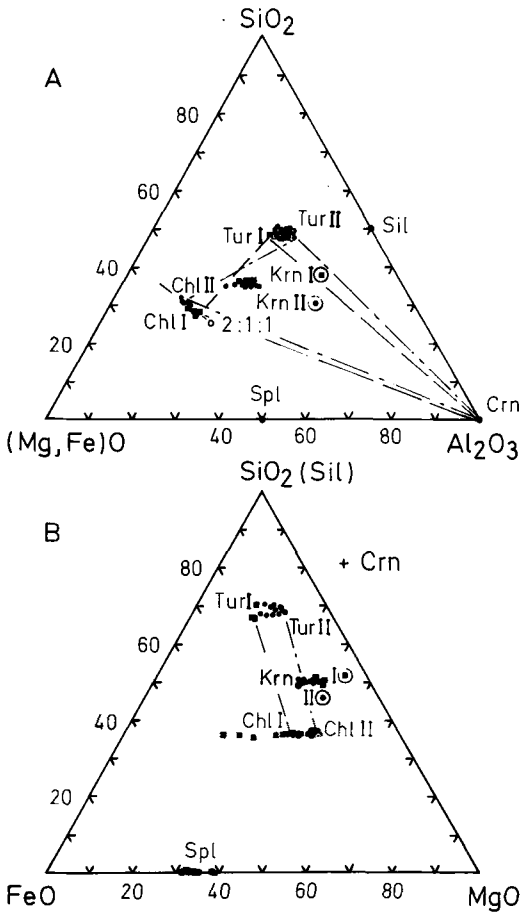

FIG. 4. Triangular diagrams in terms of the components FMAS(H) illustrating the chemical range of relevant phases: A, (Mg,Fe)O–Al_2O_3–SiO_2; B, FeO–MgO–SiO_2 as a projection from Al_2O_3.

No. 209; Spl, No. 202; Tur I, No. 210; Chl I, No. 216 and Crn, No. 208) and the sixth phase FeO (for Fe oxide) combined with the four components FeO, MgO, Al_2O_3 and SiO_2:

46 Krn (I) + 93 Spl = 29 Chl I + 5 Tur I + 120 Crn (I)

The original boundary between the kornerupine and spinel indicated in Fig. 3B and C has been derived from textural relations. Fe oxide in the centre of the reaction area, identified as hematite, is assumed to be a remnant of magnetite which had formed lamellae in spinel. Using the reaction mass balance, we suggest that the Fe oxide did not take part in the reaction. This would imply that exsolution in spinel occurred prior to the formation of the reaction texture.

Profile C–D (Fig. 5B) illustrates reaction II, that took place within one grain of kornerupine (see Fig. 3A and C). Kornerupine (Krn (II)) is bordered by the product phase chlorite (Chl II), within which there is a narrow zone of corundum, not seen here. In the centre of this reaction area there is a tourmaline (Tur II) aggregate that includes corundum.

The reaction coefficients were calculated with the six phases Krn (II) (see Table 1, No. 292), Spl, Tur II (No. 297), Chl II (No. 295), Crn (No. 290) and FeO (for Fe oxide), and the four components FeO, MgO, Al_2O_3, SiO_2:

3 Krn (II) = 1 Chl II + 1 Tur II + 3 Crn (II)

P–T conditions

Although the Beraketa belt extends along strike for at least 300 km, we use assemblages within a range of only 45 km to constrain ambient *P–T* conditions. Relevant assemblages are:

Cordierite-bearing paragneiss. Early coexistent spinel and quartz are now separated by cordierite rimming spinel. Application of the cordierite–spinel–quartz geobarometer can, therefore, only give minimum pressures (Seifert and Schumacher, 1986). Using their X_{Mg}–*P* relations 700 °C and analyses of more than 10 mineral pairs per locality we obtain P = 6.9–7.2 kbar for locality 10 (the kornerupine occurrence) decreasing to P = 6.1–6.8 at locality 11, to P = 6.0–6.5 kbar at locality 14 and finally P = 5.0–6.0 kbar at locality 16 (Fig. 1).

For coexisting garnet–cordierite–sillimanite–quartz the calculated pressure values according to the barometers of Thompson (1976) and Wells (1979) range from 7.0 to 7.5 kbar at locality 10, decreasing to 6.8–7.2 kbar at 11, to 7.3 kbar at 14, and to 6.2–6.9 kbar at 16. Although these absolute pressure data are subject to rather large uncertainties, because of the unknown role of fluids, they support a continuous decrease of pressure towards the NNW or an increase of water activity in this direction.

With a fixed P of 7 kbar, garnet–cordierite from locality 10 gives a temperature of 650–710 °C (equations given by Thompson, 1976, and Holdaway and Lee, 1977). Values from locality 14 fall into the same temperature range, and those from locality 11 range from 670 to 740 °C.

Pyroxenite. Clinopyroxene–orthopyroxene from the pyroxenite gives a temperature range of 690–750 °C for locality 14 and 710–780 °C for locality 15 (Powell, 1978; Wells, 1977).

In summary, the above *P–T* estimates suggest that P decreases from 7.0 to 5.0 kbar from south

Table 2. Representative point analyses of minerals in associated rock types

Rock type	Cordieritite		Grt-gneiss			Grt-Crd-gneiss				Pyroxenite			
Sample no.	11-6		14-1			10-3				14-3			
	Crd	Sil	Grt	Spl	Sil	Grt	Spl	Crd	Sil	Cpx	Opx	Hbl	Scp
SiO_2	49.17	36.72	38.74	-	35.80	36.80	-	48.60	35.75	51.43	54.48	41.83	48.29
TiO_2	-	0.02	0.07	-	0.02	0.04	-	-	0.02	0.34	0.08	1.93	0.02
Al_2O_3	33.09	61.65	21.64	59.59	63.06	22.02	60.27	33.83	62.55	2.86	0.94	11.10	26.30
Cr_2O_3	-	0.09	0.02	0.42	-	0.15	0.24	-	0.02	-	0.05	0.03	0.06
FeO*)	5.94	1.12*)	27.34	29.73	0.87*)	27.63	29.24	4.47	1.14*)	8.48	19.08	13.40	0.20
MnO	0.09	0.04	3.02	0.65	-	4.19	0.52	0.19	0.05	0.33	0.74	0.14	-
MgO	10.15	-	8.69	8.97	0.03	8.03	9.65	11.20	0.01	13.08	24.62	12.15	0.06
CaO	0.03	-	0.86	0.01	-	1.19	0.02	-	-	22.69	0.37	11.84	15.72
Na_2O	0.11	-	-	-	-	-	-	0.08	-	0.35	-	1.07	3.51
K_2O	0.01	-	-	-	-	-	-	-	-	0.01	-	2.79	-
Total	98.59	99.64	100.38	99.37	99.78	100.05	99.94	98.37	99.54	99.57	100.36	96.28	94.16
X_{Mg}**)	0.75	-	0.34	0.35	-	0.31	0.37	0.81	-	0.73	0.69	0.62	-
X_{Mg} (Ø)**) from	0.74-	-	0.33-	0.32-	-	0.30-	0.34-	0.80-	-	0.72-	0.65-	0.60-	-
to	-0.78		-0.38	-0.39		-0.37	-0.36	-0.85		-0.76	-0.70	-0.73	

*: Total Fe usually calculated as FeO; Fe in Sil as Fe_2O_3

**: $X_{Mg} = Mg / (Mg + Fe^{2+} + Mn)$; (Ø) average is calculated with more than ten point analyses

to north over 45 km slightly across strike, and that T is within the same range close to 700 °C; this is consistent with granulite-facies P–T conditions.

Discussion

The mineral compositions depart from the model system MgO–Al_2O_3–SiO_2–H_2O (MASH) on account of significant $Mg \rightleftharpoons Fe^{2+}$ substitution an the presence of the B_2O_3-bearing phases kornerupine and tourmaline. The components Na_2O and CaO are only present in the product phase tourmaline, and therefore must have been introduced by a fluid phase. During the P–T history of these rocks the Fe^{2+}/Fe^{3+} ratio must have changed to produce, for example, hematite from magnetite. There are significant amounts of Fe^{3+} in corundum and sillimanite, but only minor amounts in the spinel. Fe^{3+} is probably also a component of kornerupine and tourmaline, but cannot be calculated from microprobe data in these minerals.

To a first approximation let us consider the composition of the coexisting minerals in a four-component system: FeO–MgO–Al_2O_3–SiO_2–(H_2O). At the start sillimanite and spinel were stable together with an unknown silica-rich phase (perhaps cordierite). Kornerupine possibly crystallized by the reaction:

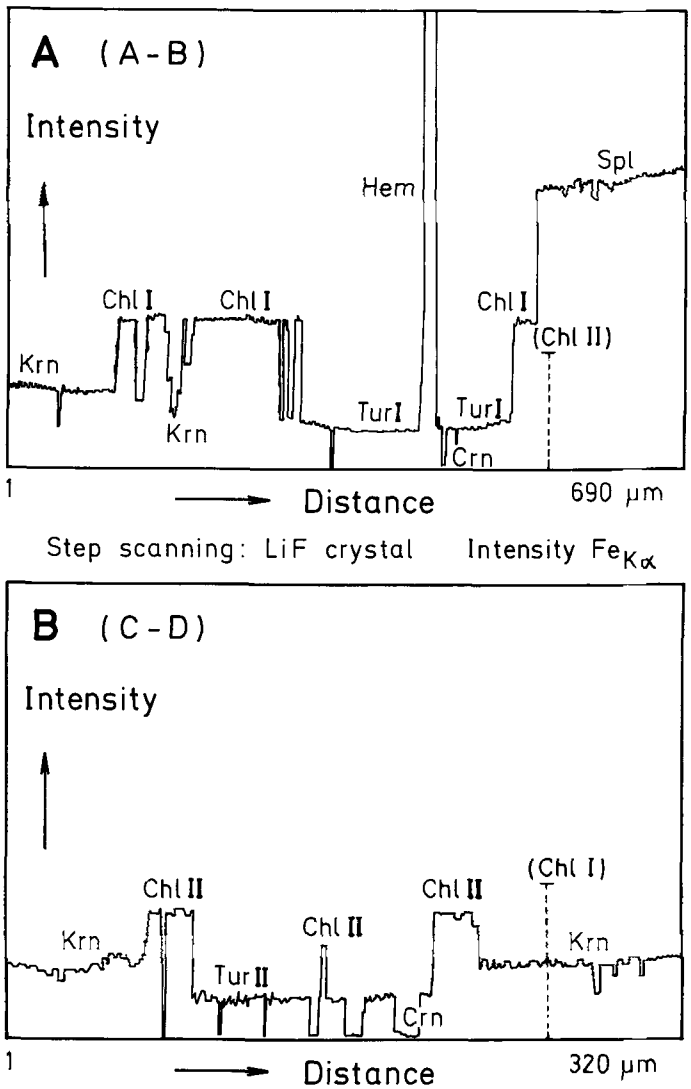

FIG. 5. Variation in iron content across the reaction areas shown in Fig. 3C obtained as electron probe Fe-*K* profiles A–B and C–D. The intensity is plotted against distance based on analysis points at 1 µm intervals. A, Reaction I: Krn (I) + Spl = Tur I + Chl I + Crn; B, Reaction II: Krn (II) = Tur II + Chl II + Crn.

$$\text{Spl} + \text{Sil} + ??? = \text{Krn} + \text{Mag}$$

in connection with B-bearing fluids.

Spinel + kornerupine were stable at granulite-facies metamorphism and then reacted according to (I):

$$\text{Krn (I)} + \text{Spl} = \text{Chl I} + \text{Tur I} + \text{Crn},$$

followed by the breakdown of kornerupine suggested by the reaction II:

$$\text{Krn (II)} = \text{Chl II} + \text{Tur II} + \text{Crn}$$

(see Ackermand *et al.*, 1984). With the continuous sequence of stages there was a change in the chemical composition of the phases which took part in the reactions. The kornerupine became progressively enriched in Al_2O_3 and FeO, whilst the chlorite became poorer in Al_2O_3 and FeO, and the spinel was enriched in FeO. The change in composition of these reacting phases led to a quasi-degenerate situation in which kornerupine (Krn II) lies on the tie-line between chlorite (Chl II) and tourmaline (Tur II).

Reactions I and II have not been previously described. Let us compare these natural reactions described in the model system FMASH with

experimentally known reactions in the system MASH. Reaction I is similar to the experimentally determined reaction (Seifert, 1975) MASH system:

Krn + sapphirine = Chl + Crn (in MASH).

Reaction II, which in the FMASH system is degenerate, may be compared with the experimentally determined reaction:

Krn = Crd + Chl + Crn (in MASH).

Reactions involving sapphirine in the Beraketa belt several km north of Imanombo (Ackermand *et al.*, 1989) demonstrate a retrograde, nearly isothermal, *P–T* trajectory starting at 10 kbar and 950 °C. From associated rocks we calculate in this paper a *P–T* condition of 7.0 kbar and 700 °C, and from relevant experimental data we infer that the earliest kornerupine-bearing assemblage was stable at this *P–T* condition. Correlation with the experimental data of Seifert (1975) suggests that the two kornerupine breakdown reactions considered to be analogous to those observed here are approximately parallel to the pressure axis, and therefore the two reactions in the natural rocks should proceed with decreasing temperature, or they are due to an increase in water fugacity, or to an increase in Na_2O activity, or to a combination of such effects.

Finally, micron-step reaction profiles are a useful way of discovering fine-grained phases not easily recognisable with the optical microscope, and they provide a means of following in detail the chemical changes across micron-size reaction boundaries.

Acknowledgements

DA and BFW are grateful to NATO for research grant no. 289.81 for study of the petrology of sapphirine-bearing rocks. BFW thanks The Royal Society for a field expedition grant, DA the Deutsche Forschungsgemeinschaft for grant AC 38/2-1; furthermore DA and AHR acknowledge the financial support by Stiftung Volkswagenwerk I/64 306. We were ably guided in the field by Th. Razakamanana, and we thank C. Chopin, E. Grew, B. Hensen, S. Lonker, R. K. Herd and F. Seifert for constructive, useful reviews.

References

Ackermand, D., Herd, R. K., and Windley, B. F. (1984) Kornerupine replacement reactions involving tourmaline, Fiskenaesset region, W. Greenland. *Neus Jahrb. Mineral., Mh.*, 490–500.

—— Windley, B. F., and Razafiniparany, A. H. (1989) The Precambrium mobile belt of Southern Madagascar. In *Metamorphic Mobile Belts* (J. S. Daly, R. A. Cliff and B. W. D. Yardley, eds.) Geol. Soc. London, Spec. Publ. No. 43, pp. 293–6.

Besairie, H. (1970) *Carte géologique No. 8; Ampanihy*, 1:500000. Service Géologique, Madagascar.

——(1971) *Carte géologique au 1/2 000 000 et notice explicative.* Documentation du Bureau Géologique, Madagascar, No. 184.

Cahen, L. and Snelling, N. J. (1984) *The Geochronology and Evolution of Africa.* Clarendon Press, Oxford 512 p.

Finger, L. W. and Burt, D. M. (1972) REACTION: A Fortran IV computer programm to balance chemical reactions. *Carnegie Inst. Washington Yearbook*, **62**, 616–20.

Grew, E. S. (1980) Sillimanite and ilmenite from high-grade metamorphic rocks of Antarctica and other areas. *J. Petrol.*, **21**, 39–68.

—— and Hinthorne, J. R. (1983) Boron in sillimanite. *Science*, **221**, 547–9.

Holdaway, M. J. and Lee, S. M. (1977) Fe–Mg cordierite in high-grade pelitic rocks based on experimental, theoretical and natural observations. *Contrib. Mineral. Petrol.*, **63**, 175–98.

Hottin, G. (1976) Présentation et essai d'interprétation du Precambrien de Madagascar. *Bull. Bureau de Récherche Géologique et Minère*, Paris, 2nd Series, **4**, no. 2, 117–53.

Knorring, O. von, Sahama, T. G., and Lehtinen, M. (1969) Kornerupine-bearing gneiss from Inanakafy near Betroka, Madagascar. *Bull. Geol. Sci. Finland*, **41**, 79–84.

Kretz, R. (1983) Symbols for rock-forming minerals. *Am. Mineral.*, **68**, 277–9.

Lacroix, A. (1922–3) *Minéralogie de Madagascar.* E. Challamel, Paris, 3 vols.

——(1941) Les gisements de phlogopite de Madagascar. *Comptes Rendus Sem. Géol. de Madagascar*, 27–37.

Megerlin, N. (1968) Sur une roche à kornerupine du sud de Ianakafy (Centre sud de Madagascar). Ibid., 67–9.

Nicollet, C. (1988) *Metabasites granulitiques, anorthosites et roches associées de la croute inférière: Exemples pris à Madagascar et dans le Massif Central français.* Thèse d'Etat, Université Blaise Pascal, Clermont-Fd, No. d'ordre 413, 315 pp.

——(1990) Occurrence of grandidierite, serendibite, and tourmaline near Ihosy, southern Madagascar. *Mineral. Mag.*, **54**, 131–3.

Noizet, G. (1969) *Contribution à l'étude géologique des formation métamorphiques du faciè granulite dans le Sud de Madagascar.* Thèse d'Etat, Université Nancy.

Pouchou, J. L. and Pichoir, F. (1984) A new model for quantitative X-ray microanalysis. Part I: Application to analysis of homogeneous samples. *La Récherche Aérospatiale*, **3**, 13–36.

Powell, R. (1978) The thermodynamics of pyroxene geotherms. *Phil. Trans. Roy. Soc. London*, **A288**, 457–69.

Seifert, F. (1975) Boron-free kornerupine: a high-pressure phase. *Am. J. Sci.*, **275**, 57–87.

—— and Schumacher, J. C. (1986)

Cordierite–spinel–quartz assemblages: a potential geobarometer. *Bull. Geol. Sci. Finland*, **58**, 95–108.

Thompson, A. B. (1976) Mineral reactions in pelitic rocks. *Am. J. Sci.*, **276**, 401–24, and 425–54.

Wells, P. R. W. (1977) Pyroxene thermometry in simple and complex systems. *Contrib. Mineral. Petrol.*, **62**, 129–39.

——(1979) Chemical and thermal evolution of Archaean sialic crust, southern Greenland. *J. Petrol.*, **20**, 187–226.

[*Manuscript received 15 January 1990; revised 13 June 1990*]